Biochemistry

pubs.acs.org/biochemistry Article

Unraveling the RNA Binding Properties of the Iron−Sulfur Zinc Finger Protein CPSF30

Jordan D. Pritts, Matthew S. Hursey, Jamie L. Michalek, Sharon Batelu, Timothy L. Stemmler, and Sarah L. J. Michel*

Cite This: *Biochemistry* 2020, 59, 970−982 Read Online

ACCESS | Metrics & More | Article Recommendations | Supporting Information

ABSTRACT: Cleavage and polyadenylation specificity factor 30 (CPSF30) is a "zinc finger" protein that plays a crucial role in the transition of pre-mRNA to RNA. CPSF30 contains five conserved CCCH domains and a CCHC "zinc knuckle" domain. CPSF30 activity is critical for pre-mRNA processing. A truncated form of the protein, in which only the CCCH domains are present, has been shown to specifically bind AU-rich pre-mRNA targets; however, the RNA binding and recognition properties of full-length CPSF30 are not known. Herein, we report the isolation and biochemical characterization of full-length CPSF30. We report that CPSF30 contains one 2Fe−2S cluster in addition to five zinc ions, as measured by inductively coupled plasma mass spectrometry, ultraviolet−visible spectroscopy, and X-ray absorption spectroscopy. Utilizing fluorescence anisotropy RNA binding assays, we show that full-length CPSF30 has high binding affinity for two types of pre-mRNA targets, AAUAAA and polyU, both of which are conserved sequence motifs present in the majority of pre-mRNAs. Binding to the AAUAAA motif requires that the five CCCH domains of CPSF30 be present, whereas binding to polyU sequences requires the entire, full-length CPSF30. These findings implicate the CCHC "zinc knuckle" present in the full-length protein as being critical for mediating polyU binding. We also report that truncated forms of the protein, containing either just two CCCH domains (ZF2 and ZF3) or the CCHC "zinc knuckle" domain, do not exhibit any RNA binding, indicating that CPSF30/RNA binding requires several ZF (and/or Fe−S cluster) domains working in concert to mediate RNA recognition.

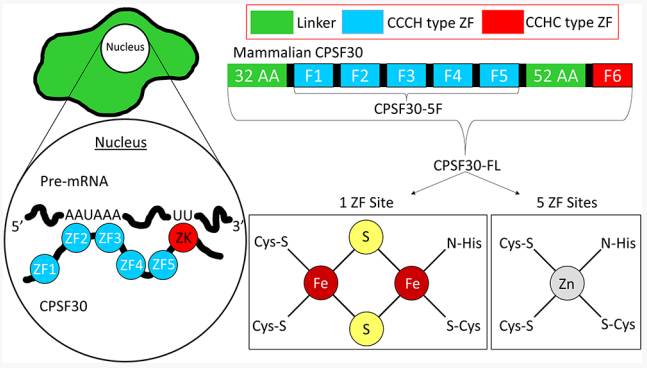

Zinc finger (ZF) proteins are proteins that contain domains with conserved repeats of cysteine and histidine residues. These residues serve as ligands to coordinate zinc, thereby allowing the domain to adopt a folded structure that is functional.[1−5] Initially identified as transcription factors, ZFs are now known to facilitate numerous biological processes ranging from signal transduction to membrane association.[1,2,6−9] It has been estimated that 3−10% of all eukaryotic proteins are ZFs, and more recently, a small number of ZFs have been identified in prokaryotes and archaea.[10] These estimates for the ubiquity of ZFs come principally from sequence data, and to confirm that proteins annotated as ZFs from proteomics projects are bona fide zinc finger proteins, they must be studied experimentally.[11,12]

ZFs can be categorized into different classes or families based upon the number of cysteine (C) and histidine (H) residues (e.g., CCHH, CCCH, CCCC, etc.) within each ZF domain, as well as the spacing between residues and/or known structures.[1,4,7,10,13−15] One important class is the CCCH class of ZFs. These proteins are often associated with RNA processing events, and the handful that have been characterized biochemically have been shown to be RNA binding proteins, typically targeting adenine/uracil-rich RNA sequences.[1,4,15−17]

One member of the CCCH family of ZF proteins that plays a critical biological role is cleavage and polyadenylation specificity factor 30 (CPSF30, also known as CPSF4). CPSF30 is part of a complex of proteins (CPSF160, CPSF100, CPSF30, FIP1, and WDR33), collectively termed the cleavage and polyadenylation specificity factor (or CPSF). CPSF facilitates the transition of RNA from pre-mRNA to mRNA.[2,18−23] This transition involves the removal of a 3′ polyuracil (polyU) sequence present in the pre-mRNA strand, after which a 3′ polyadenine (polyA) sequence is added (Figure 1A). The molecular-level details of how each CPSF protein modulates this important biological transition are not fully understood.

Received: December 5, 2019
Revised: February 5, 2020
Published: February 6, 2020

https://dx.doi.org/10.1021/acs.biochem.9b01065
Biochemistry 2020, 59, 970−982

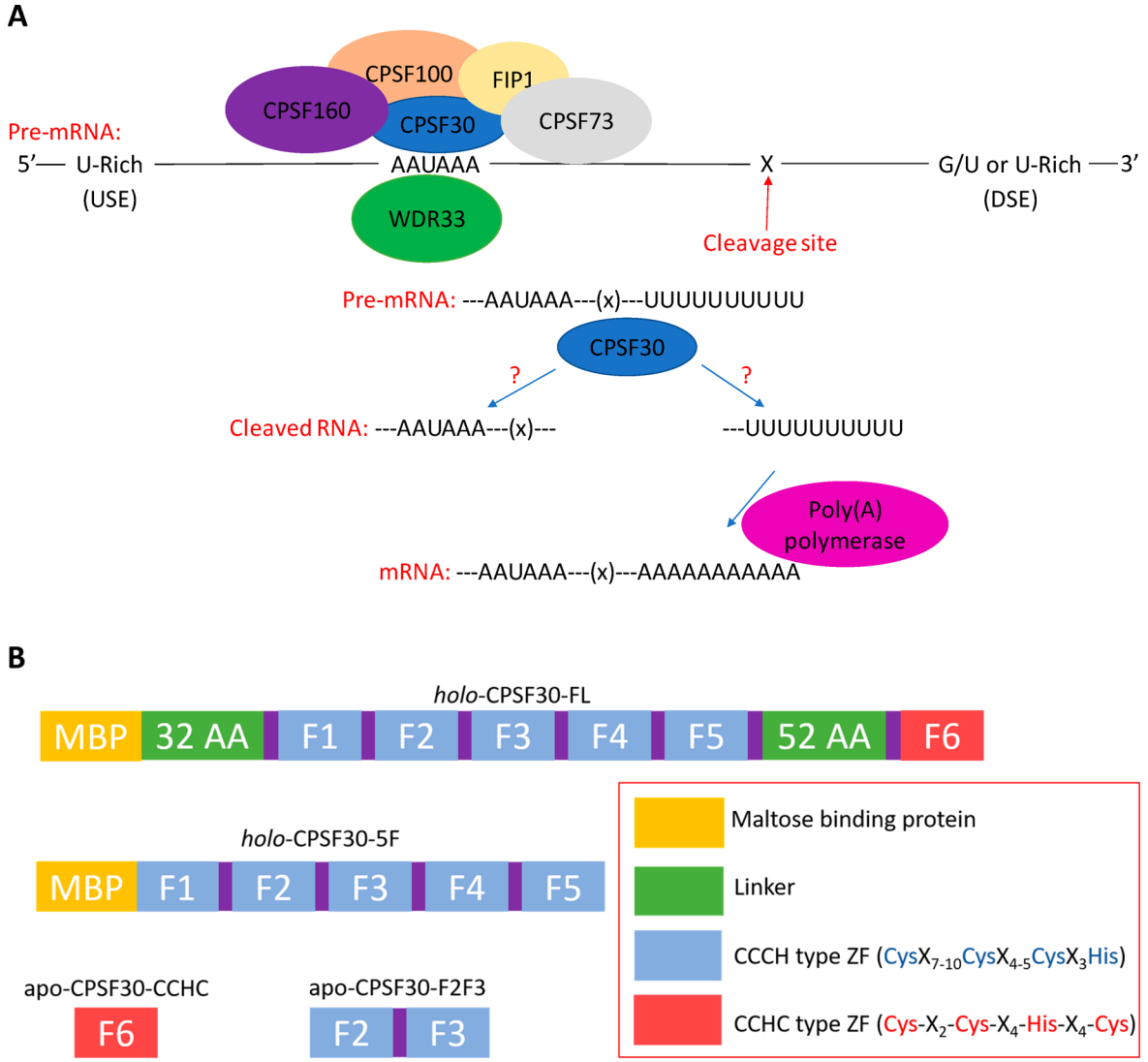

Figure 1. (A) Cartoon diagram of CPSF30 function. (B) Diagram of CPSF30 constructs investigated in this work.

Mammalian CPSF30 contains five CCCH domains and one CCHC domain (often termed a "zinc knuckle" domain). CPSF30 was initially annotated as a zinc finger protein based upon the presence of the CCCH domains; however, when we isolated a truncated construct of CPSF30, containing just the five CCCH domains [CPSF30-5F (Figure 1B)], we discovered that the protein contains a 2Fe−2S cluster in addition to zinc.[18] This Fe−S cluster was determined to be coordinated to one of the CCCH "zinc finger" domains. This discovery that an annotated "zinc finger" protein (CPSF30) binds an Fe−S cluster at one of the "zinc finger" domains adds to a growing number of proteins that have been discovered to house Fe−S clusters, despite being annotated as "CCCH" type zinc fingers. These proteins include Miner, mitoNEET, MiNT, and Fep1, underscoring the need to study annotated ZFs experimentally.[24−31]

We also determined that the truncated CPSF30-5F functions as an RNA binding protein. CCCH type zinc fingers often recognize AU-rich RNA sequences, and we found that the five-CCCH domain construct selectively recognizes the polyadenylation signal (PAS, AAUAAA) present in most pre-mRNAs and the binding interaction best fits to a cooperative binding model (Figure 1A).[18] Notably, we discovered that for high-affinity RNA binding CPSF30-5F must be loaded with both the 2Fe−2S cluster and zinc, suggesting a role of the 2Fe−2S cluster in RNA recognition.[18] Subsequently, two cryo-electron microscopy (cryo-EM) structures of CPSF30 complexed with other CPSF proteins (CPSF-160 and WDR33) along with a short RNA strand containing the PAS (AAUAAA) were reported.[32,33] In the structure reported by Sun et al., full-length CPSF30 protein was utilized, while in the structure reported by Clerici et al., a truncated form containing ZF1−ZF5 (residues 1−178) was utilized. In both structures, only the first three CCCH domains of CPSF30 were visible, and the focus of the work was not on the zinc sites so the zinc atoms were not modeled in with constraints. In addition, in the cryo-EM structures, a singular CPSF30 and a singular RNA strand are present, suggesting that the cooperativity that we measure for CPSF30-5F/RNA via fluorescence anisotropy binding may reflect sequential domain binding to RNA, rather than dimerization. Nonetheless, these structures provided a snapshot of part of the multiprotein CPSF complex and revealed that in addition to CPSF30, WDR33 binds RNA, while CPSF-160 is involved in protein−protein interactions with WDR33 and CPSF30. In the cryo-EM structures, ZF2 and ZF3 from CPSF30 directly bind to RNA, suggesting that

https://dx.doi.org/10.1021/acs.biochem.9b01065
Biochemistry 2020, 59, 970−982

in the context of the full-length protein, these domains determine RNA recognition. It is not known whether the two CCCH domains alone are sufficient for protein/RNA binding.

CPSF30 also contains a CCHC domain, often called a "zinc knuckle" domain, at the 3′ end that is not present in the cryo-EM structures. The function of this domain has not yet been elucidated. Much like CCCH domain proteins, zinc knuckle domain proteins are often involved in RNA binding, albeit to G/C- and U-rich targets instead of AU-rich targets.[34−37] Most pre-mRNAs contain a conserved U-rich sequence that aids in efficient processing from pre-mRNA to mRNA.[38−41] We therefore hypothesized that the CPSF30 "zinc knuckle" domain binds the pre-mRNA U-rich element while the CCCH domains bind to the AU-rich PAS signal.

Herein, we tested the hypothesis that the CPSF30 "zinc knuckle" domain binds the pre-mRNA U-rich element by overexpressing and purifying the full-length CPSF30 protein and determining its RNA binding properties. We report that full-length CPSF30 is isolated and active with one 2Fe−2S cluster and five zinc cofactors. Notably, we show that full-length CPSF30 binds to polyuracil RNA with high affinity, in addition to binding to the PAS (AAUAAA) sequence. These results demonstrate, for the first time, that isolated CPSF30 binds to polyuracil sequences. In contrast, CPSF30-5F (which lacks the zinc knuckle domain) does not bind to polyuracil RNA, binding to only the PAS, providing clear evidence that the zinc knuckle domain of CPSF30 is required for polyuracil RNA binding. Additionally, we produced the single zinc knuckle domain of CPSF30 (CPSF30-ZK) and evaluated its ability to bind to polyuracil RNA. No binding to polyuracil RNA was observed for the CPSF30-ZK, revealing that the zinc knuckle domain alone is not sufficient for RNA binding and that other domain elements within CPSF30 are involved in polyuracil RNA binding.

We also sought to characterize the role of ZF2 and ZF3 in binding to the PAS sequence. In the published cryo-EM structures of CPSF30, the ZF2 and ZF3 domains are in contact with the PAS, suggesting that these two domains are critical for RNA binding.[32,33] Often proteins with CCCH domains require just two structured domains for high-affinity binding to AU-rich RNA targets, as is the case with tristetraprolin; therefore, a construct of CPSF30 with just ZF2 and ZF3 has the potential to be sufficient for binding.[42,43] We report studies focused on this truncated protein, which reveal that ZF2 and ZF3 alone are not capable of binding to the PAS hexamer in the absence of the other ZF domains. From these collective data, a mechanism for PAS and polyU RNA binding by CPSF30 that involves multiple ZF domains and specific RNA sequence elements is proposed.

MATERIALS AND METHODS

Materials. $ZnCl_2$, $FeCl_3$, Na_2S nonahydrate, ampicillin sodium salt, KCl, polycytidylic acid, bovine serum albumin (BSA), $ZnSO_4$, urea, trifluoroacetic acid (TFA) [high-performance liquid chromatography (HPLC) grade], methanol (HPLC grade), SP sepharose resin, glycerol, and RNA (HPLC-purified grade) were obtained from Sigma-Aldrich. Isopropyl β-D-1-thiogalactopyranoside (IPTG) was purchased from Research Products International. BL21-DE3 competent cells and amylose resin were acquired from New England Biolabs. Luria-Bertani Lennox Broth (LB) and dithiothreitol (DTT) were obtained from American Bio. Glucose was purchased from Calbiochem. Tris base [2-amino-2-(hydroxymethyl)propane-1,3-diol], NaCl, nitric acid (trace metal grade), acetonitrile (HPLC grade), and hydrochloric acid (trace metal grade) were acquired from Fisher Scientific. Iron, zinc, germanium, and scandium inductively coupled plasma mass spectrometry (ICP-MS) standards were obtained from Fluka analytical. The bismuth ICP-MS standard was purchased from Ricca Chemical Co. The rhodium ICP-MS standard was acquired from VWR analytical. The ICP-MS tuning solution was obtained from Agilent. MES was acquired from Amresco. Tris(2-carboxyethyl)phosphine (TCEP) and protease and phosphatase inhibitor tablets were obtained from Thermo Scientific. 4,4′-Dithiodipyridine (DTDP) was purchased from Acros Organics. $CoCl_2$ was acquired from Merck.

Table 1. RNA Oligomers Utilized in This Study[a]

RNA oligomer	RNA sequence (5'-3')
α-syn$_{30}$	UCUCACUUUAAUAAUAAAAAUCAUGCUUAU
α-syn$_{24}$	CACUUUAAUAAUAAAAAUCAUGCU
PolyC$_{24}$	CACUUUAAUCCCCCCAAUCAUGCU
ΔA$_{1,2,4,5}$	CACUUUAAUCCUCCAAAUCAUGCU
PolyU$_{24}$	UUUUUUUUUUUUUUUUUUUUUUUU
ARE$_{11}$	UUUAUUUAUUU
AAU$_9$	AAUAAUAAU
AAU$_{12}$	AAUAAUAAUAAU
AAU$_{24}$	AAUAAUAAUAAUAAUAAUAAUAAU

[a]The polyadenylation sequence and subsequent mutations are underlined.

General Considerations. Extra care was taken to ensure that all reagents remained metal free throughout each experiment. Water was purified using a PURELAB flex ultrapure water system and then purified further over chelex resin to ensure the chelation of any contaminating metal ions.

Molecular Cloning, Expression, and Purification of Holo-CPSF30-FL. DNA from the *Bos taurus* CPSF30 homologue was from G. Martin and W. Keller (University of Basel, Basel, Switzerland). DNA encoding full-length CPSF30 was cloned into the pMAL-c5e plasmid (New England Biolabs) utilizing the NdeI and BamHI restriction sites and verified using the University of Maryland Baltimore's Biopolymer-Genomics core facility.

Full-length CPSF30 was cloned into the pMAL-c5e plasmid (holo-CPSF30-FL). BL21-DE3 competent *Escherichia coli* cells were transformed with holo-CPSF30-FL via heat shock. Transformed cells were incubated for 45 min at 37 °C. Overnight cultures containing 50 mL of LB broth (Lennox) with 100 μg/mL ampicillin were inoculated with 150 μL of transformed BL21-DE3 cells. The next day 10−15 mL of overnight culture was utilized to inoculate 1 L of LB broth (Lennox) containing 100 μg/mL ampicillin and 0.2% (w/v) glucose. At an optical density of ∼0.3, cultures were supplemented with 0.8 mM $ZnCl_2$ and 0.6 mM $FeCl_3$. Cell cultures were grown at 37 °C until the OD_{600} reached 0.5−0.6, where protein expression was induced with 1 mM IPTG and the medium was supplemented with 0.4 mM $Na_2S{\cdot}9H_2O$. Protein expression was allowed to continue for 3 h at 37 °C, after which the cells were pelleted at 7800*g* and 4 °C for 20 min and stored at −20 °C. Pellets were resuspended in 20 mM Tris and 200 mM NaCl (pH 7.5) with a protease and phosphatase inhibitor tablet (Thermo Scientific). Resuspended

https://dx.doi.org/10.1021/acs.biochem.9b01065
Biochemistry 2020, 59, 970−982

pellets were lysed by sonication and centrifuged at 17710*g* and 4 °C for 20 min. The sonicated supernatant was spiked with an additional 300 mM sodium chloride, loaded onto the amylose column in a final buffer containing 20 mM Tris and 500 mM NaCl (pH 7.5), and incubated at room temperature for 15−20 min while being shaken. The supernatant was then allowed to flow through the column. The salt concentration was gradually decreased to a final concentration of 200 mM through subsequent washes. Protein elution was conducted in 20 mM Tris, 200 mM NaCl, and 30 mM maltose (pH 7.5). The ultraviolet−visible spectrum of the isolated holo-CPSF30-FL protein was measured, after which the protein was concentrated via centrifugation utilizing a 30 kDa molecular weight cutoff spin filter. The protein concentration was determined by utilizing the calculated extinction coefficient, ε, of 88200 M^{-1} cm^{-1} at 278 nm, and the protein purity was verified via sodium dodecyl sulfate polyacrylamide gel electrophoresis (SDS−PAGE). CPSF30 was then buffer exchanged into either 20 mM Tris and 100 mM NaCl (pH 8.0) for fluorescence anisotropy studies or 20 mM Tris and 50 mM NaCl (pH 7) for X-ray absorption spectroscopy (XAS) studies utilizing a 30 kDa molecular weight cutoff spin filter. Protein purity and metal loading were verified using SDS−PAGE and ICP-MS, respectively.

Molecular Cloning, Expression, and Purification of Holo-CPSF30-5F. Holo-CPSF30-5F was cloned, expressed, and purified as previously described by our laboratory with the following exceptions.[2,18] During protein expression, 0.8 mM $ZnCl_2$ and 0.6 mM $FeCl_3$ were added to the expression flasks at an OD_{600} of ∼0.3, and 0.4 mM $Na_2S{\cdot}9H_2O$ was added at an OD_{600} of 0.5−0.6 where the cultures were then induced with the addition of 1 mM IPTG. The protein concentration was determined as for holo-CPSF30-FL except a calculated extinction coefficient of 85400 M^{-1} cm^{-1} at 278 nm was utilized and the protein purity was verified via SDS−PAGE.

Fluorescence Anisotropy (FA) Studies of Holo-CPSF30. The binding of CPSF30 to RNA was measured using fluorescence anisotropy (FA). Binding studies were performed using an ISS K2 spectrofluorometer configured in the L-format with an excitation wavelength and slit width of 495 nm and 2 mm, respectively, and an emission wavelength and slit width of 517 nm and 1 mm, respectively. A 5 mm pathlength quartz fluorometer cuvette contained 500 μL of 5 nM 3′ 6-carboxyfluorescein (6-FAM) fluorescently labeled RNA in 50 mM Tris, 100 mM KCl, 0.3 mg/mL polycytidylic acid, and 0.1 mg/mL BSA, and the mixture was equilibrated in each cuvette for 5 min. The RNA oligomers utilized were purchased from MilliporeSigma at HPLC-purified grade. Their sequences are listed in Table 1.

For a typical titration, CPSF30 was titrated into a cuvette containing fluorescently labeled RNA, and the change in FA was monitored until saturation. After each addition of protein, the sample was allowed to equilibrate for 5 min. FA titrations were conducted in triplicate, and each data point comprised 60 readings taken over 115 s. A single replicate positive control of CPSF30 with the canonical RNA target (α-syn30 or α-syn24) was conducted in tandem with all titrations to ensure that the protein in use was fully active. Prior to data analysis, raw anisotropy values were corrected for changes in the quantum yield of the fluorophore using the equation[18]

$$r_c = \frac{r_0(r_b - r) + rQ(r - r_0)}{r_b - r + Q(r - r_0)}$$

where r_c is the corrected anisotropy, r is the raw anisotropy, r_0 is the anisotropy of the free fluorescently labeled RNA, and r_b is the anisotropy of the RNA−protein complex at saturation. The corrected anisotropy was plotted against protein concentration and analyzed using a cooperative binding model programmed into GraphPad Prism 5:

$$nP + R \rightleftharpoons P_nR$$

$$K = \frac{[P_nR]}{[P]^n[R]}$$

$$r_{tc} = r_0 + (r_b - r_0)\frac{\left(\frac{[P]}{[P]_{1/2}}\right)^h}{1 + \left(\frac{[P]}{[P]_{1/2}}\right)^h}$$

where r_{tc} is the total corrected anisotropy, $[P]$ is the protein concentration, $[P]_{1/2}$ is the protein concentration at which half of the protein ensemble is saturated, and h is the Hill coefficient.

Inductively Coupled Plasma Mass Spectrometry (ICP-MS). ICP-MS was performed as previously described with the following exceptions.[2,18] Protein samples were diluted to 1 μM in 6% trace metal grade nitric acid to a final volume of 2 mL. An internal standard solution of Bi, Ge, Rh, and Sc was run in line through a mixing T to the nebulizer at an inner diameter of 1/10 of the sample line. All samples were measured in He mode to avoid interference with argon oxide.

X-ray Absorption Spectroscopy (XAS). CPSF30 samples were prepared in a 20 mM Tris, 50 mM NaCl, 30% glycerol buffer (pH 7), with metal concentrations of ∼0.7 mM Fe and ∼2.0 mM Zn. Protein samples were loaded into prewrapped 2 mm Leucite XAS cells, flash-frozen, and then stored in liquid nitrogen until X-ray exposure. Fe and Zn K-edge XAS data were collected at the Stanford Synchrotron Radiation Lightsource (SSRL) on beamline 9-3, equipped with a Si[220] double-crystal monochromator with an upstream mirror for X-ray focusing and harmonics rejection. Samples were maintained at 10 K using an Oxford Instruments continuous-flow liquid helium cryostat. Fluorescence spectra were recorded using a Canberra 100-element germanium solid state detector. Solar slits and a 3 μm Mn or 3 μm Cu layer (for Fe or Zn analysis, respectively) were placed between the cryostat and detector to diminish random fluorescence scattering and remove low-energy background signals. All XAS spectra were recorded in 5 eV increments within the pre-edge region, with 0.25 eV increments in the edge region. EXAFS data were collected in 0.05 $Å^{-1}$ increments, out to k = 14 $Å^{-1}$, integrated from 1 to 25 s in a k^3-weighted manner during data collection. The total XAS scan length was ∼40 min. Fe and Zn foil absorption spectra were simultaneously recorded with each respective protein spectrum, for spectral calibration, and the first inflection point energy was set at 7111.2 eV for Fe and 9659 eV for Zn.

XAS spectra were processed and analyzed using the EXAFSPAK program suite written for Macintosh OS-X.[44] EXAFSPAK is integrated with Feff version 8[45] for theoretical model generation. Normalized X-ray absorption near-edge spectral (XANES) data for Fe data were subjected to pre-edge and edge analysis. Iron 1s → 3d pre-edge peak analysis was completed following our established protocol,[46] and pre-edge peak areas were determined over the energy range of 7110−

https://dx.doi.org/10.1021/acs.biochem.9b01065
Biochemistry 2020, 59, 970−982

7116 eV. The iron oxidation state was deduced by comparing first inflection edge energies from Fe protein samples to our Fe(II) and Fe(III) model library.[47] In the extended X-ray absorption fine structure (EXAFS) region, data collected to k = 14 Å^{-1} correspond to a spectral resolution of 0.12 Å^{-1} for all metal−ligand interactions.[47] As a result, only independent scattering environments at distances of >0.12 Å were considered resolvable during fitting analysis. Data were fit using both single- and multiple-scattering amplitudes and phase model functions to simulate iron and zinc metal−oxygen/nitrogen, metal−sulfur, and metal−metal interactions. During Fe data simulations, a scale factor (Sc) of 0.95 and threshold shift (ΔE_0) values of −10 eV (Fe−O/N/C), −12 eV (Fe−S), and −15 eV (Fe−Fe) were used; for Zn simulations, an Sc of 0.9 and E_0 values of −15.25 eV (Zn−O/N/C and Zn−S) were used. These calibration values were obtained from fitting crystallographically characterized small molecule Fe and Zn compounds,[46,48] and these values were held constant during spectral simulations. The best-fit EXAFS simulation for each sample was based on the lowest mean square deviation value (F'),[49] measured between data and simulated spectra, corrected for the number of degrees of freedom in the simulation, and using an acceptable Debye−Waller value (between 0.0001 and 0.006 Å^2) for each ligand environment.[48] During simulations, only the bond length and Debye−Waller factor for each ligand environment were allowed to freely vary; coordination numbers were held constant but manually stepped incrementally at half-integer values to help identify the optimal spectral simulation parameters.

Purification of Apo-CPSF30-ZK. A peptide corresponding to the C-terminal zinc knuckle domain of CPSF30 was purchased from Bio-Synthesis Inc. (Lewisville, TX). The peptide sequence was QVTCYKCGEKGHYANRCTKG. This sequence length was modeled after other CCHC domains [nucleocapsid protein (NCp7), T4 gene protein 32 (gp32), and the nucleic acid binding protein encoded by the *Drosophila* Fw- element].[50−53] For a typical experiment, 5 mg of the peptide stock was resuspended in ELGA PURELAB flex purified water and then incubated with 5 mM TCEP at room temperature for 1 h. Following incubation, the peptide was purified using reverse-phase high-performance liquid chromatography (RP-HPLC) under nonmetallic conditions (Waters 600 assembled with peak tubing and a Symmetry prep C18 7 μm column). A gradient beginning with 90% water containing 0.1% trifluoroacetic acid (TFA) mixed and 10% acetonitrile containing 0.1% TFA was utilized to separate the apo-CPSF30-ZK from any contaminants, with apo-CPSF30-ZK eluting in a single peak at 80% water/0.1% TFA and 20% acetonitrile/0.1% TFA. Upon collection of apo-CPSF30-ZK, the peptide was transferred to an anaerobic chamber where it was lyophilized and stored in a solid form. The peptide mass was confirmed using matrix-assisted laser desorption ionization time-of-flight (MALDI-TOF) mass spectrometry. All further peptide manipulations were completed anaerobically. All buffers were thoroughly degassed with argon prior to use. Cuvettes used for ultraviolet−visible (UV−vis) spectroscopy were designed with screw-capped Teflon-sealed lids for anaerobic work.

UV−Vis Co(II) Titrations with Apo-CPSF30-ZK. For a typical titration, 100 μM peptide was used. The titrations involved the addition of cobaltous chloride, in increments determined by molar equivalents. For apo-CPSF30-ZK titrations, $CoCl_2$ additions were as follows: 0.1, 0.2, 0.3, 0.4, 0.5, 0.6, 0.8, 1, 2, 5, 10, and 20 equiv as each titration point. Each set of titrations was carried out in triplicate. Co(II) coordination resulted in the appearance of d−d transition bands between 500 and 800 nm. The following maximum absorbance peaks were observed for Co(II)−CPSF30-ZK: 608 nm (shoulder), 645 nm, and 700 nm. The data at 650 nm, where the d−d envelope maximum is observed, were plotted against the concentration of $CoCl_2$ added. The data were then fit to a 1:1 binding equilibrium using Kaleidagraph software (Synergy Software) and nonlinear least-squares analysis.

$$\mathrm{P} + \mathrm{Co(II)} \overset{K_d^{Co}}{\longleftrightarrow} \mathrm{Co(II)-P}$$

$$\text{therefore: } K_d^{Co} = \frac{[\mathrm{P}][\mathrm{Co(II)}]}{[\mathrm{Co(II)-P}]}$$

$$[\mathrm{PCo(II)}] = [\mathrm{P}]_T + [\mathrm{Co(II)}]_T + K_d\sqrt{([\mathrm{P}]_T + [\mathrm{Co(II)}]_T + K_d)^2 - 4[\mathrm{P}]_T[\mathrm{Co(II)}]_T}$$

where [P] is the apoprotein concentration.

Binding of Zinc to CPSF30-ZK. The relative affinity of CPSF30-ZK for Zn(II) was determined by monitoring the displacement of Co(II) by Zn(II) following the method developed by Berg and Merkle.[42,43,54] The data were then fit to a competitive binding equilibrium.

Fluorescence Anisotropy Studies of Zn(II)−CPSF30-ZK. The zinc knuckle's ability to bind U-rich RNA was assessed utilizing a fluorescence anisotropy binding assay. Prior to FA binding studies, the active concentration of the peptide was determined utilizing the extinction coefficient of CPSF30-ZK with excess cobalt at 650 nm. Peptide concentrations for FA were corrected for activity, and stoichiometric amounts of zinc were added to the apopeptide (between 100 and 500 μM) under anaerobic conditions, forming the Zn-coordinated peptide. Zn(II)−CPSF30-ZK was titrated into 5 mm fluorometer quartz cuvettes containing 50 mM Tris, 100 mM NaCl, 0.3 mg/mL polycytidylic acid, 0.1 mg/mL BSA, and 5 nM 3′ 6-FAM-labeled RNA. Both ARE_{11} and $polyU_{24}$ RNAs were evaluated. During each experiment, the solution was allowed to equilibrate for 5 min after titrating in peptide and mixing. FA measurements comprised of 60 readings over a total time of 115 s.

Molecular Cloning, Expression, and Purification of CPSF30-F2F3. A construct for CPSF30, named CPSF30-F2F3, which encodes the second and third ZF domains of CPSF30, with a sequence of "AISGEKTVVCKHWLRGLCKKGDQCEFLHEYDMTKMPECYFYSKFGECSNKECPFLHIDPESK", was overexpressed and purified. CPSF30-F2F3 was cloned into the pET-15b expression vector. BL21-DE3 competent *E. coli* cells (New England Biolabs) were then transformed with CPSF30-F2F3 via heat shock. The cells were grown in LB broth (Lennox) medium with 100 μg/mL ampicillin at 37 °C until mid-log phase (OD_{600} = 0.6−0.8) before being induced with 1 mM IPTG. After cultures were allowed to grow for 4 h postinduction, cells were harvested by centrifugation at 7800g and 4 °C for 15 min. Cell pellets were resuspended in 8 M urea and 10 mM MES (pH 5.0) with a Pierce EDTA free protease and phosphatase inhibitor mini tablet (Thermo Scientific). The cells were lysed by sonication on ice; 1 mM DTT was added, and cells were centrifuged at 12100 rpm and 4 °C for 15 min. The resulting supernatant was added to a SP Sepharose gravity column and incubated by being rocked for 60 min at room temperature. A NaCl step

https://dx.doi.org/10.1021/acs.biochem.9b01065
Biochemistry 2020, 59, 970−982

gradient was used, ranging from 0 to 2 M, in 4 M urea and 10 mM MES (pH 5.0), with each wash containing 10 mM DTT. To prepare for further purification, 25 mM DTT was added, and the solution was heated in a water bath at 56 °C for 2 h, followed by filtration (Millipore 0.22 μM Steriflip). The supernatant was then applied to a C18 reverse-phase HPLC column (Symmetry 300 C18 Prep 5 μm, 19 mm × 150 mm column) on an Agilent Technologies 1200 Series LC system, and a water/acetonitrile [H_2O/CH_3CN, 0.1% trifluoroacetic acid (TFA)] gradient was applied. Purified CPSF30-F2F3 eluted at 28% CH_3CN. The protein identity was confirmed via SDS−PAGE and MALDI-TOF mass spectrometry. Further handling of purified CPSF30-F2F3 was done anaerobically in a Coy anaerobic chamber (3% H_2 and 97% N_2).

UV−Vis Co(II) and Zn(II) Binding Assays for Apo-CPSF30-F2F3. The affinity of CPSF30-F2F3 for cobalt and zinc was determined by spectrophotometrically monitoring the titration of apo-CPSF30-F2F3 with $CoCl_2$ until saturation. The relative affinity for Zn(II) was determined by titrating Co-CPSF30-F2F3 with $ZnCl_2$ and monitoring the displacement of Co(II) spectrophotometrically via the method of Berg and Merkle.[54] The experiments were performed in 200 mM HEPES, 100 mM NaCl buffer (pH 7.5). Titrations were performed by titrating 0−20 equiv of $CoCl_2$ incrementally and then titrating $ZnCl_2$ in a similar fashion.

Fluorescence Anisotropy Binding Assays for CPSF30-F2F3. Six 3′ 6-carboxyfluorescein (6-FAM)-labeled RNA oligonucleotides purchased from MilliporeSigma (HPLC-purified grade) were utilized for these studies (Table 1). FA experiments were performed on an ISS k2 multifrequency phase fluorimeter with an excitation wavelength of 495 nm and an emission wavelength of 517 nm. The buffer system consisted of 200 mM HEPES, 50−100 mM NaCl, and 0.05 mg/mL BSA (pH 7.5 and 8.0) using 5−10 nM RNAs ARE_{11}, AAU_9, AAU_{12}, AAU_{24}, α-syn_{24}, and α-syn_{30}. Zn(II)−CPSF30-F2F3 was titrated into cuvettes containing the buffer system and the RNA, up to 1.2 μM protein, while the anisotropy was monitored.

Circular Dichroism (CD) Studies of CPSF30-F2F3. Circular dichroism (CD) was utilized to assess the secondary structure of apo-CPSF30-F2F3 and Zn(II)−CPSF30-F2F3 on a Jasco-810 spectropolarimeter. The CD spectra were scanned from 280 to 180 nm at a rate of 50 nm/min, with a bandwidth of 1 nm and a sensitivity of 100 mdeg. Each spectrum shown represents an average of three accumulations. A 1 mm path-length quartz cuvette was utilized, and the temperature was maintained at 25 °C. A 15.5 μM solution of apo-CPSF30-F2F3, made in 10 mM sodium phosphate buffer at pH 7.5, was scanned first. To the 15.5 μM solution of apo-CPSF30-F2F3, 2.0 equiv of $ZnCl_2$ was added and the CD spectrum was recorded.

RESULTS AND DISCUSSION

Full-Length CPSF30 Contains Iron and Zinc. Full-length CPSF30 contains a zinc knuckle domain with unknown function, in addition to five CCCH domains that we, and others, have previously shown are involved in binding to the PAS, AAUAAA.[2,18,20,32,33,55] Zinc knuckle domains are often present in RNA binding proteins involved in viral replication (e.g., HIV nucleocapsid protein) and often recognize G/C- and U-rich sequence elements.[37] In addition to a conserved AAUAAA sequence, most pre-mRNAs contain a conserved polyuracil sequence. To determine the role of the zinc knuckle domain of CPSF30 in RNA binding and to delineate whether it binds to polyuracil sequences, full-length CPSF30 was overexpressed and purified. Like its five-CCCH domain counterpart (CPSF30-5F), full-length CPSF30 turned red upon overexpression, suggesting the presence of an iron cofactor.[18] The UV−vis spectrum of CPSF30 exhibits absorbance peaks at 420 and 456 nm, which are indicative of a 2Fe−2S cluster and match those observed for CPSF30-5F (Figure 2, inset).[18] Metal occupancy was confirmed by utilizing inductively coupled plasma mass spectrometry (ICP-MS). The presence of both iron and zinc, ranging from 0.69 to 1.51 equiv and from 3.08 to 4.69 equiv (minimum to maximum), respectively, suggests that the full-length protein contains a singular 2Fe−2S cluster and five zinc sites.

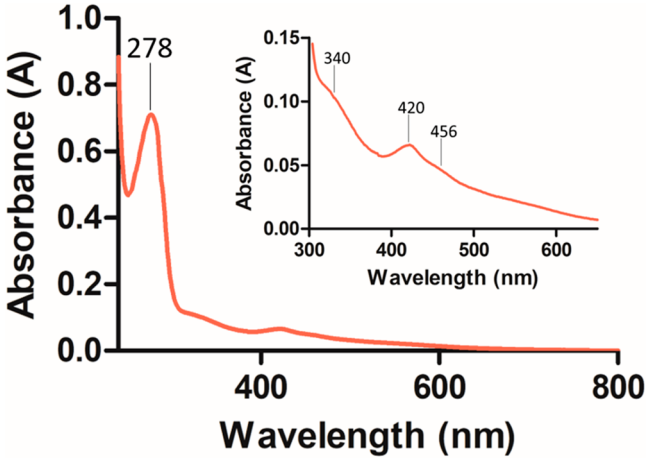

Figure 2. UV−visible spectrum of CPSF30-FL in 20 mM Tris and 100 mM NaCl (pH 8) between 240 and 800 nm with the maximum protein peak at 278 nm indicated. The inset shows a close-up of the spectrum between 300 and 650 nm with peak maxima indicated.

X-ray Absorption Spectroscopy (XAS) of the Iron and Zinc Sites. XAS was used to characterize the iron−ligand metrical parameters in Fe- and Zn-loaded CPSF30. The iron k-edge XANES spectrum is shown in Figure 3 with an inset that displays the expanded 1s → 3d pre-edge spectral signal. XANES data provide direct insight into the metal oxidation state, and the XANES pre-edge region provides insight into the metal−ligand bond symmetry and spin state for iron. The sharp/defined pre-edge spectral feature seen at 7112.8 eV in the Fe-CPSF30 XANES is characteristic of low-spin iron existing in a tetrahedral ligand conformation. The pre-edge peak area, determined to be 0.051 eV^2, is consistent with values we obtained for Fe−S cluster centers in several proteins.[46] The excitation energy of the first inflection point in the Fe XANES, measured at 7122.22 eV, is consistent with an oxidized Fe(III)−S cluster.[46] Simulations of the Fe EXAFS for CPSF30 (Figure 4) indicated an Fe−nearest neighbor coordination environment constructed by 1.5 ± 1 oxygen/nitrogen ligands centered at a distance of 2.01 Å and a second, more dominate, Fe−ligand environment of 2 ± 1 sulfur atoms centered at 2.27 Å. The appearance of a distinct Fe···Fe ligand vector at 2.69 Å is characteristic of scattering observed for Fe−S clusters.[46] Long range scattering is also observed for carbon atoms positioned at an average distance of 3.92 Å from the central iron (Table 2).

XAS was further used to characterize the Zn−ligand metrical parameters for the Zn in the Fe/Zn-loaded CPSF30 sample. The first inflection point energy in the Zn XANES occurs at

https://dx.doi.org/10.1021/acs.biochem.9b01065
Biochemistry 2020, 59, 970−982

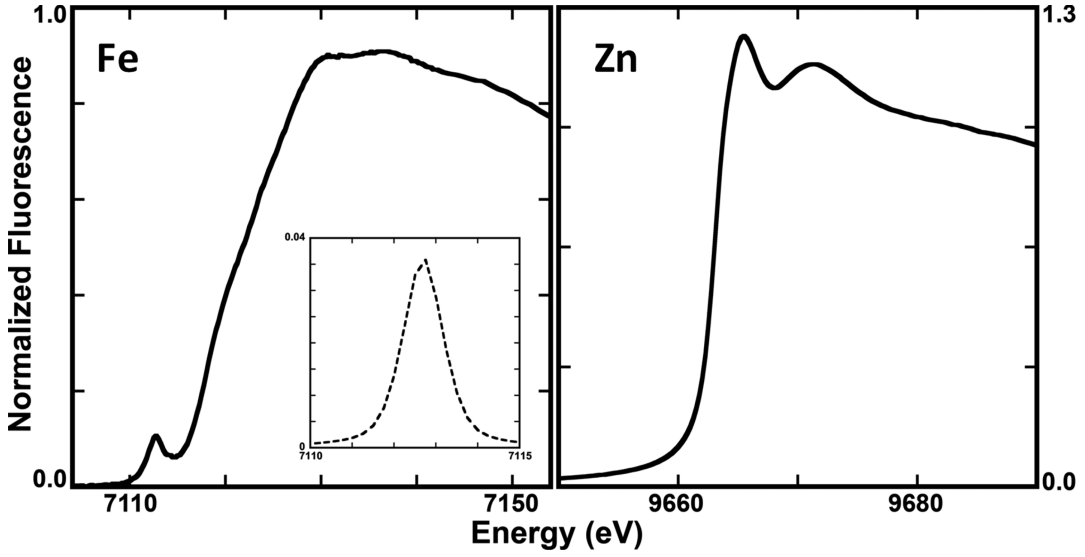

Figure 3. Normalized XANES spectra Fe/Zn-loaded CPSF30: (left) Fe-XANES spectrum, with the 1s → 3d pre-edge inset, and (right) Zn-XANES spectrum.

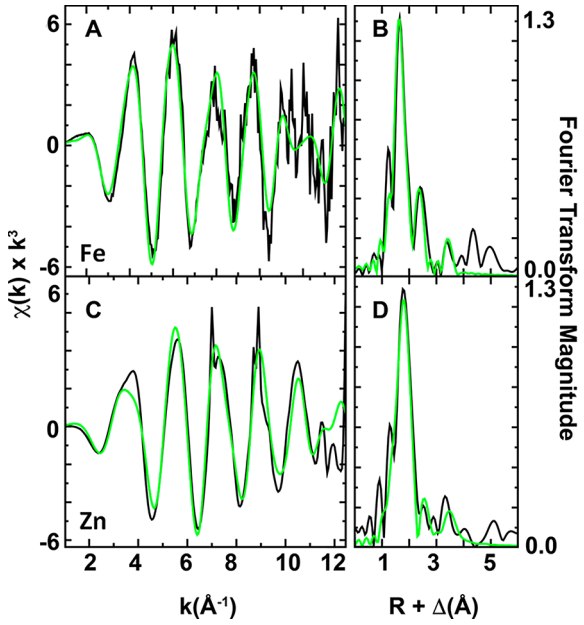

Figure 4. EXAFS and Fourier transforms (FTs) of the EXAFS for Fe/Zn-loaded CPSF30. Iron EXAFS, and FT of the EXAFS, for Fe/Zn-loaded CPSF30 are shown in panels A and B, respectively. Zinc EXAFS, and FT of the EXAFS, for Fe/Zn-loaded CPSF30 are shown in panels C and D, respectively. Best-fit spectral simulations are colored green.

9663 eV, consistent with Zn(II) metal. The excitation edge shows two distinct features in the peak maximum at 9665.2 and 9671.9 eV, characteristic of environments that include independent sulfur and oxygen/nitrogen ligand scattering, environments similar to those previously found in ZnN_1S_3 peptide XAS.[56,57] The Zn EXAFS region was best simulated with 1 ± 1 Zn−O/N ligand at a distance of 2.06 Å and 3 ± 1 Zn−S atoms at an average distance of 2.31 Å. Two long range carbon ligation environments were also observed at average distances of 3.15 and 3.95 Å, respectively (Table 2). Collectively, the UV−vis, ICP-MS, and XAS data indicate that full-length CPSF30 is a "zinc finger" protein with a 2Fe−2S cofactor, with all metal sites binding to a 3Cys/1His ligand set from the protein.

RNA Binding: Full-Length CPSF30 Binds to Polyuracil Sequences and the Polyadenylation Signal (AAUAAA) in a Cooperative Manner. With full-length CPSF30 isolated, we sought to determine its RNA binding properties. CCCH domains typically bind to AU-rich RNA targets, and the five-CCCH domain construct, CPSF30-5F, binds to the AAUAAA PAS hexamer; on the contrary, zinc knuckle domains bind to various RNA target sequences, with a preference for G/C- and U-rich targets.[15,34−37,42,43] Most pre-mRNAs contain a polyU sequence, and there is some evidence from radiolabeled in vitro translation experiments that CPSF30 interacts with polyU sequences bound to sepharose resin.[34] Because CPSF30 contains both CCCH and CCHC domains, we predicted that the protein would recognize both AU-rich and U-rich

Table 2. Summary of the Fe and Zn EXAFS Simulation Results for Fe/Zn-Loaded CPSF30

	nearest neighbor ligands[a]				long range ligands[a]				
metal	atom[b]	R (Å)[c]	CN[d]	σ^2[e]	atom[b]	R (Å)[c]	CN[d]	σ^2[e]	F'[f]
Fe	O/N	2.01	1.5	0.5	Fe	2.69	0.5	2.6	1.2
	S	2.27	2.0	5.1	C	3.92	2.0	1.4	
Zn	O/N	2.06	1.0	5.7	C	3.15	3.0	4.7	1.0
	S	2.31	3.0	3.4	C	3.95	3.0	1.2	

[a]Independent metal−ligand scattering environment. [b]Scattering atoms: N (nitrogen), O (oxygen), C (carbon), and S (sulfur). [c]Average metal−ligand bond length. [d]Average metal−ligand coordination number. [e]Average Debye−Waller factor (×10³ Å²). [f]Number of degrees of freedom weighted mean square deviation between data and fit.

https://dx.doi.org/10.1021/acs.biochem.9b01065
Biochemistry 2020, 59, 970−982

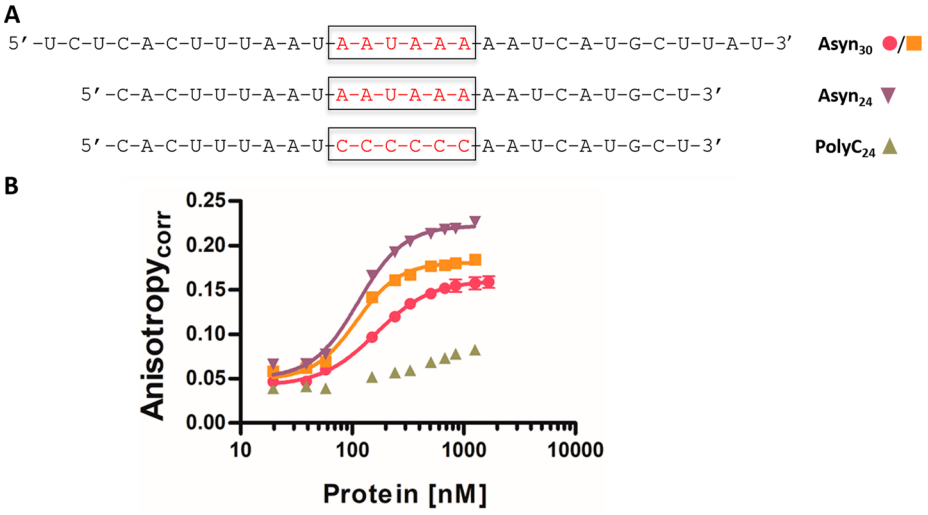

Figure 5. (A) Sequences of α-synuclein 30mer (α-syn$_{30}$), α-synuclein 24mer (α-syn$_{24}$), and polyC 24mer (polyC$_{24}$) RNAs. (B) Fluorescence anisotropy (FA)-monitored binding of holo-CPSF30-FL to α-syn$_{30}$ (orange squares), holo-CPSF30-FL to α-syn$_{24}$ (purple triangles), holo-CPSF30-5F to α-syn$_{30}$ (pink circles), and holo-CPSF30-FL to polyC$_{24}$ (green triangles). An average of three representative titrations is plotted, and the error is shown as the standard error of the mean (SEM). Data are fit to a cooperative binding model.

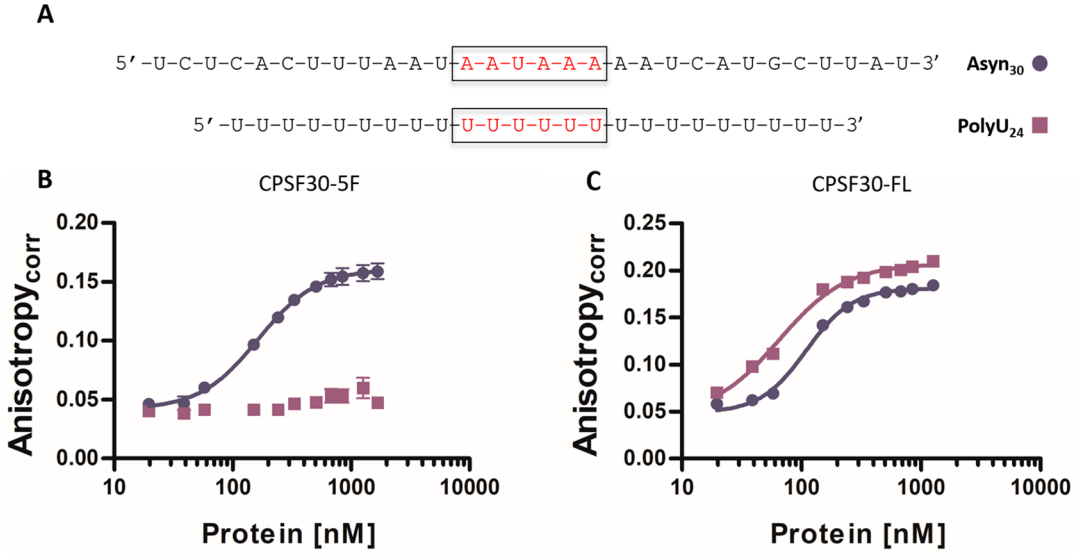

Figure 6. (A) Sequences of α-synuclein 30mer (α-syn$_{30}$) and polyU 24mer (polyU$_{24}$) RNAs. (B) FA-monitored binding of holo-CPSF30-5F and α-syn$_{30}$ (blue circles) and holo-CPSF30-5F and polyU$_{24}$ (purple squares). (C) FA-monitored binding of holo-CPSF30-FL and α-syn$_{30}$ (blue circles) and holo-CPSF30-FL with polyU$_{24}$ (purple squares). An average of three representative titrations is plotted, and the error is shown as the standard error of the mean (SEM). Data are fit to a cooperative binding model.

targets. To investigate this prediction, we determined the interaction of full-length CPSF30 with AU-rich RNA and polyU-rich RNA via fluorescence anisotropy (FA). Our initial experiments focused on an AU-rich RNA sequence from α-synuclein, α-syn$_{30}$ and α-syn$_{24}$ (30 and 24 bases in length, respectively), that we had previously reported binds to the five-ZF construct of CPSF30, CPSF30-5F.[18] The titration of full-length CPSF30 with either α-syn$_{30}$ or α-syn$_{24}$ resulted in a binding curve that was best fit to a cooperative binding model with $[P]_{1/2}$ values of 109.5 ± 11.1 nM [mean ± standard error of the mean (SEM)] and 110.3 ± 14.0 nM and Hill coefficients of 2.3 and 2.1 for the 30mer and 24mer, respectively. This affinity is slightly tighter than the affinity for the truncated five-finger CPSF30 construct (CPSF30-5F) to α-syn$_{30}$ ($[P]_{1/2}$ of 177.6 ± 23.6 nM and Hill coefficient of 1.8) (Figure 5). To determine if the binding observed for CPSF30-FL involves the AU hexamer, CPSF30-FL was titrated with a variant of the α-syn$_{24}$ sequence in which that AU hexamer was modified to all cytosines (polyC$_{24}$) (Figure 5). No binding was observed, indicating that the AU hexamer is required for binding of full-length CPSF30 to pre-mRNA. We note that the same result was observed for the five-finger CPSF30 construct, CPSF30-5F, suggesting that the CCCH domains are directly involved in binding to the AU hexamer.[18]

We then sought to understand if the full-length CPSF30 protein interacts with polyU sequences, via its zinc knuckle domain. In pre-mRNA, a U/GU-rich cis-acting downstream element (DSE) is located 35−45 nucleotides downstream of the PAS, and together, these elements aid in stimulating polyadenylation.[58] Therefore, a compelling hypothesis is that CPSF30 binds to both the PAS and the polyU sequence via its distinct CCCH and CCHC domains. To determine CPSF30's

https://dx.doi.org/10.1021/acs.biochem.9b01065
Biochemistry 2020, 59, 970−982

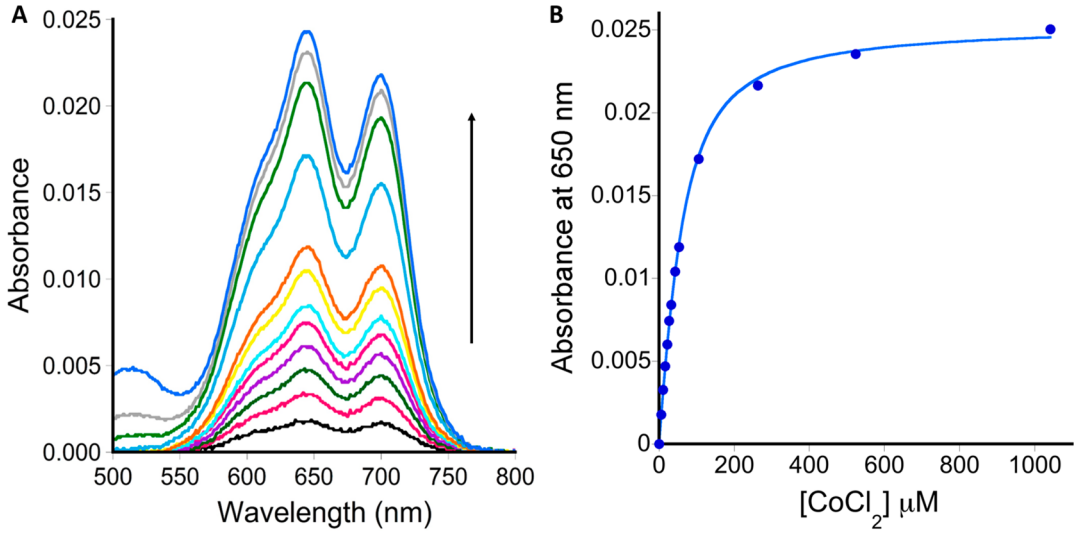

Figure 7. (A) Plot of the change in absorption as apo-CPSF30-ZK is titrated with $CoCl_2$. The experiment was conducted in 200 mM MES buffer at pH 6.0. (B) Plot of the change in the absorption spectrum at 650 nm as a function of concentration as Co(II) is added to apo-CPSF30-ZK. The data were fit to yield an upper limit dissociation constant, K_d, of $(3.08 \pm 0.12) \times 10^{-7}$ M. The solid line represents a nonlinear least-squares fit to a 1:1 binding model.

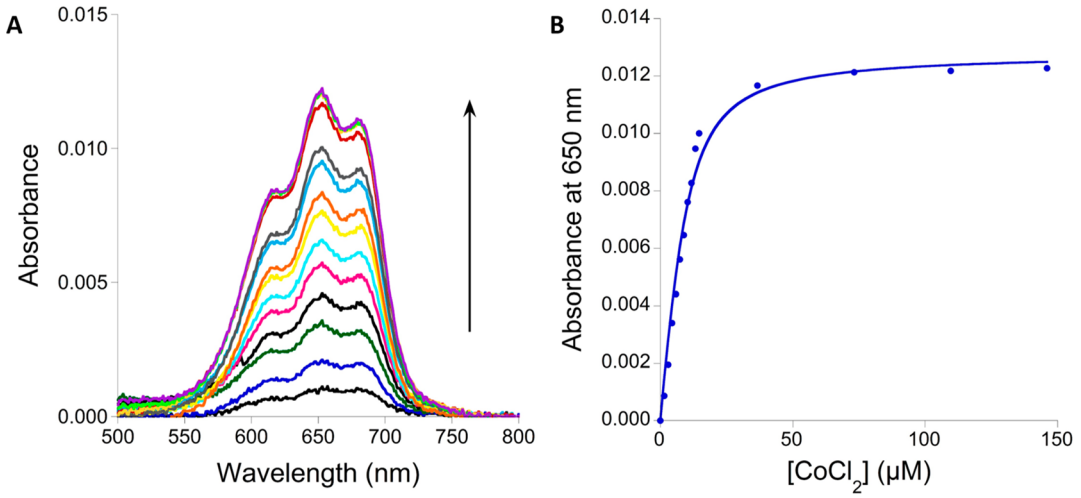

Figure 8. (A) Plot of the change in absorption as apo-CPSF30-F2F3 is titrated with $CoCl_2$. The experiment was performed in 200 mM HEPES buffer and 100 mM NaCl at pH 7.5. (B) Plot of the change in the absorption spectrum at 650 nm as a function of concentration as cobalt(II) is added to apo-CPSF30-F2F3. The data were fit to yield an upper limit dissociation constant, K_d, of $(2.01 \pm 1.08) \times 10^{-6}$ M. The solid line represents a nonlinear least-squares fit to a 1:1 binding model.

RNA binding properties, an FA experiment of full-length CPSF30 with a polyU sequence was performed. A titration of CPSF30 with polyU RNA resulted in a clear binding isotherm, with an affinity of 65.0 ± 3.0 nM and a Hill coefficient of 1.5 when fit to a cooperative binding equilibrium (Figure 6). Notably, the CPSF30 construct with only the five CCCH domains does not exhibit any affinity for the polyU sequence, revealing that the CCHC domain is required for this interaction. Together, these data reveal that full-length CPSF30 directly binds to polyU RNA.

The Zinc Knuckle Domain, CPSF30-ZK, Binds Cobalt and Zinc but Not Polyuracil RNA. Our finding that the five-CCCH domain construct of CPSF30 (CPSF30-5F) does not bind to polyuracil sequences while the addition of a zinc knuckle domain (full-length CPSF30) promotes high-affinity binding to a polyuracil sequence suggested that the zinc knuckle domain itself might be sufficient for polyuracil binding. To test this hypothesis, we first had to obtain a construct of CPSF30 that contains just the zinc knuckle domain and folds around zinc. To this end, a 20-amino acid peptide that contains the CCHC "zinc knuckle" sequence was synthesized and purified in the apo form via reverse-phase HPLC. To verify that this construct binds zinc, a direct titration with Co(II), as a spectroscopic probe for the spectroscopically silent (d^{10}) Zn(II), was performed. The resultant Co(II)−CPSF30-ZK spectrum, shown in Figure 7A, exhibits d−d bands centered at 650 and 700 nm, which are indicative of a CCHC ligand set and closely resembles the cobalt spectra reported for the CCHC domains encoded within the *Drosophila melanogaster* Fw transposable element.[52] An upper limit K_d of $(3.08 \pm 0.12) \times 10^{-7}$ M was determined by fitting the data to a 1:1 binding equilibrium (Figure 7B). Typically, ZFs have a dissociation constant for Co(II) in the low-micromolar to high-nanomolar regime; therefore, the affinity measured here for Co binding to

https://dx.doi.org/10.1021/acs.biochem.9b01065
Biochemistry 2020, 59, 970−982

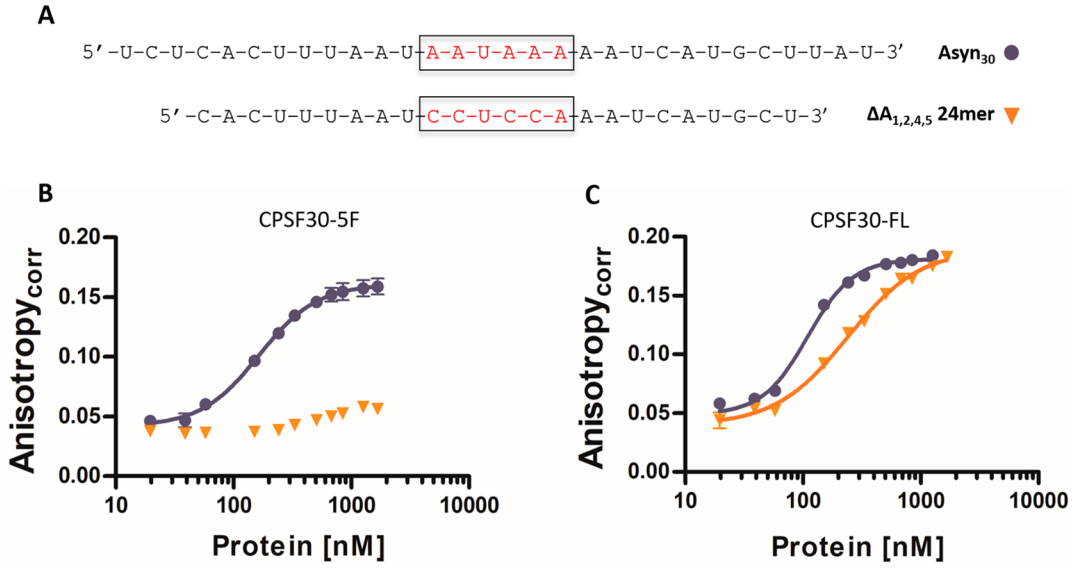

Figure 9. (A) Sequences of α-synuclein 30mer (α-syn$_{30}$) and quadruple mutant 24mer ($\Delta A_{1,2,4,5}$) RNAs. (B) FA-monitored binding of holo-CPSF30-5F and α-syn$_{30}$ (blue circles) and holo-CPSF30-5F and $\Delta A_{1,2,4,5}$ (yellow triangles). (C) FA-monitored binding of holo-CPSF30-FL and α-syn$_{30}$ (blue circles) and holo-CPSF30-FL with $\Delta A_{1,2,4,5}$ (yellow triangles). An average of three representative titrations is plotted, and the error is shown as the standard error of the mean (SEM). Data are fit to a cooperative binding model.

CPSF30-ZK fits within the values reported for other ZFs.[15,59] The calculated molar absorptivity of apo-CPSF30-ZK for Co(II) was 562 ± 34 M^{-1} cm^{-1}. ZFs typically have a molar absorptivity of 400−600 M^{-1} cm^{-1} for each tetrahedrally coordinated Co(II) center; therefore, the data obtained for the Co(II)−CPSF30-ZK construct are consistent with a tetrahedral site.[15,54,60,61]

A competitive titration with Zn was then performed to verify that Zn(II) binds to CPSF30-ZK and to determine an upper limit K_d for Zn binding. As Zn(II) was titrated with Co(II)−CPSF30-ZK, a loss of the d−d transition bands was observed, due to the displacement of the bound Co(II) ions with Zn(II).[54] These data were fit to a competitive binding equilibrium, and an upper limit dissociation constant for coordination of Zn(II) to CPSF30-ZK of (9.40 ± 0.17) × 10^{-14} M was determined (Figure S1). This affinity is consistent with the affinities of zinc for other CCHC domains.[51,52]

To determine if Zn(II)−CPSF30-ZK binds to polyuracil RNA, Zn(II)−CPSF-ZK was titrated with fluorescently labeled U-rich RNA of lengths varying from 11 to 24 nucleotides, and the fluorescence anisotropy was monitored. No change in anisotropy was observed for any of the RNA strands investigated (Figure S2). Typically, ZFs bind to target RNA or DNA with at least two domains to achieve submicromolar affinity; therefore, it is perhaps not surprising that a single ZF domain does not bind to RNA.[62,63] These data, in conjunction with the full-length CPSF30 data, reveal that the zinc knuckle domain of CPSF30 is necessary but not sufficient for binding to the polyU sequence.

Determination of the ZF2 and ZF3 Domains in CPSF30/PAS Binding. CPSF30 contains five CCCH domains, and our solution-based RNA binding studies have shown that high-affinity binding to the AAUAAA PAS sequence occurs when the five CCCH domains are present. However, CCCH ZFs often require only two domains to bind to AU-rich RNA targets. For instance, TTP binds to an AU-rich RNA target with just two CCCH domains.[42,43,62,64] Additionally, in the reported cryo-EM structures of the CPSF complex (CPSF30, CPSF160, and WDR33) with short RNA sequences (AACCUCCAAUAAACAAC and ACAAUAAAGG, respectively), the second and third ZF domains interact specifically with A1/A2 and A4/A5 within the AAUAAA PAS sequence.[32,33] Collectively, these data suggest that a construct of ZF2 and ZF3 may be sufficient for RNA binding to the PAS sequence and that residues 1, 2, 4, and 5 within the PAS hexamer are critical for RNA binding.

To determine if ZF2 and ZF3 together are sufficient for RNA binding to the PAS, a construct of CPSF30 containing only ZF2 and ZF3 was overexpressed and purified. To verify that the CPSF30-F2F3 construct binds zinc, Co(II) was used as a spectroscopic probe for zinc, as previously reported for other ZFs.[1,63] As shown in Figure 8A, as apo-CPSF30-F2F3 is titrated with Co(II), d−d transition bands centered at 615, 650, and 678 nm appear, indicative of tetrahedral coordination. An upper limit K_d of (2.01 ± 1.08) × 10^{-6} M was determined by fitting the data to a 1:1 binding model (Figure 8B). The transition bands and dissociation constant for Co(II) ions are consistent with reported values for other CCCH domains.[1,42]

A competitive titration with zinc was then performed to determine if Zn(II) binds the two-finger construct, CPSF30-F2F3. By titrating Co(II)−CPSF30-F2F3 with Zn(II), the Co(II) absorbance peaks decreased, indicating that the bound Co(II) ions were being replaced with Zn(II) (Figure S3A). The data were fit to a competitive binding model, and an upper limit K_d of (3.38 ± 2.49) × 10^{-13} M was determined for Zn(II)−CPSF30-F2F3 (Figure S3B). This affinity is consistent with the affinities reported for zinc binding to other CCCH domains.[1,42] The CD spectra of apo-CPSF30-F2F3 and Zn(II)−CPSF30-F2F3 were also obtained (Figure S4), and distinct structural changes were observed upon Zn(II) coordination indicating folding. The CD spectrum of Zn(II)−CPSF30-F2F3 is similar to that obtained for Zn(II)−TTP-2D, a CCCH zinc finger that contains two CCCH domains.[42]

To investigate if Zn(II)−CPSF30-F2F3 is sufficient to bind to the AU hexamer sequence, Zn(II)−CPSF30-F2F3 was

https://dx.doi.org/10.1021/acs.biochem.9b01065
Biochemistry 2020, 59, 970−982

titrated with six fluorescently labeled RNA targets containing AU hexamer sequences. These RNA oligomers ranged in length from 9 to 30 bases (Figure S5). To our surprise, none of the six RNAs investigated (AAU_9, AAU_{12}, AAU_{24}, ARE_{11}, α-syn_{24}, and α-syn_{30}) exhibited any binding to Zn(II)−CPSF30-F2F3, suggesting that the F2F3 construct of CPF30 is not sufficient for RNA binding and other regions of the protein; perhaps other ZF domains or an Fe−S cluster cofactor are required for RNA binding.

Role of the PAS RNA Sequence in CPSF30 Five Finger and Full-Length RNA Binding. To determine the effects of residues 1, 2, 4, and 5 within the PAS sequence (AAUAAA) on CPSF30/RNA binding, CPSF30-5F and full-length CPSF30 were titrated with an α-synuclein pre-mRNA in which adenines 1, 2, 4, and 5 within the PAS sequence were mutated to cytosines (ΔA1,2,4,5). The prediction was that these adenines are critical for CPSF30/RNA binding, and the mutation would abrogate binding. This prediction was borne out for CPSF30-5F, which did not exhibit any binding to the mutated PAS sequence. In contrast, full-length CPSF30 still bound to the mutated RNA sequence, albeit with diminished affinity (~2.5 times weaker; $[P]_{1/2}$ = 275.1 ± 37.3 nM, and Hill coefficient = 1.4), as shown in Figure 9. The mutated α-synuclein pre-mRNA still contains a U-rich sequence at the 5′ end, and therefore, because full length can bind to polyU RNA, this result further supports the role of the ZK in polyU binding.

CONCLUSIONS

Collectively, these studies reveal that full-length CSPF30 is an iron−sulfur and zinc cofactored protein that recognizes two conserved pre-mRNA sequences—AAUAAA (the PAS) and U-rich RNA—in a metal-dependent, cooperative manner. While we do not yet know the order of binding, on the basis of these results, a preliminary mechanism is shown in Figure 10, whereby the CCCH domains recognize the AAUAAA sequence and the CCHC zinc knuckle domain, in conjunction with the CCCH domain, recognize the polyuracil sequence. Notably, only CPSF30 proteins in higher eukaryotes contain CCHC domains within their sequences, suggesting that CPSF30 may have evolved to recognize two types of RNA targets in higher-order eukaryotes by connecting different types of "zinc finger" domains.[34,65] These studies elaborate the role of CPSF30 alone and contribute to our understanding of the larger CPSF complex, for which RNA binding interactions are not well understood. Studies that aim to structurally characterize the CPSF30/RNA complex to tease out the functional roles of the individual CCCH and CCHC domains are in progress.

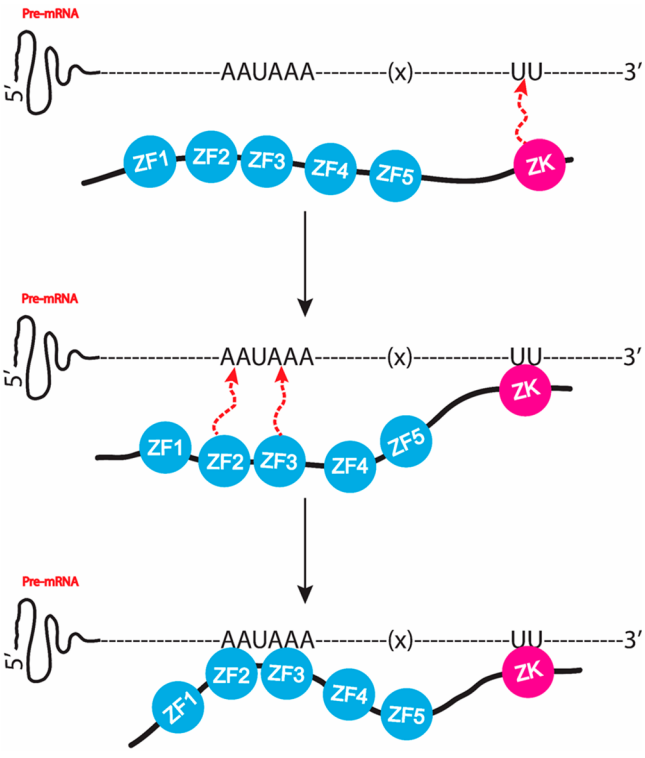

Figure 10. Preliminary RNA binding mechanism of full-length CPSF30 binding pre-mRNA.

ASSOCIATED CONTENT

Supporting Information

The Supporting Information is available free of charge at https://pubs.acs.org/doi/10.1021/acs.biochem.9b01065.

Titration of zinc with Co(II)−CPSF30-ZK, FA binding assay for binding of Zn(II)−CPSF30-ZK to RNA, zinc titration of Co(II)−CPSF30-F2F3, FA binding assay for binding of Zn(II)−CPSF30-F2F3 to RNA, and CD spectroscopy of CPSF30-F2F3 (Figures S1−S5, respectively) (PDF)

Accession Codes

CPSF30, UniProt entry O19137.

AUTHOR INFORMATION

Corresponding Author

Sarah L. J. Michel − *Department of Pharmaceutical Sciences, School of Pharmacy, University of Maryland, Baltimore, Maryland 21201-1180, United States;* orcid.org/0000-0002-6366-2453; Phone: (410) 706-7038; Email: smichel@rx.umaryland.edu; Fax: (410) 706-5017

Authors

Jordan D. Pritts − *Department of Pharmaceutical Sciences, School of Pharmacy, University of Maryland, Baltimore, Maryland 21201-1180, United States;* orcid.org/0000-0002-2806-9849

Matthew S. Hursey − *Department of Pharmaceutical Sciences, School of Pharmacy, University of Maryland, Baltimore, Maryland 21201-1180, United States*

Jamie L. Michalek − *Department of Pharmaceutical Sciences, School of Pharmacy, University of Maryland, Baltimore, Maryland 21201-1180, United States*

Sharon Batelu − *Department of Pharmaceutical Sciences, Wayne State University, Detroit, 48201, United States*

Timothy L. Stemmler − *Department of Pharmaceutical Sciences, Wayne State University, Detroit, 48201, United States*

Complete contact information is available at: https://pubs.acs.org/10.1021/acs.biochem.9b01065

Funding

S.L.J.M. is grateful for the National Science Foundation (CHE-1708732) for support of this work. T.L.M. acknowledges the National Institutes of Health (DK068139). J.D.P. acknowledges a CBI training grant (GM066706) and the AFPE for partial support.

Notes

The authors declare no competing financial interest.

REFERENCES

(1) Kluska, K., Adamczyk, J., and Krężel, A. (2018) Metal binding properties, stability and reactivity of zinc fingers. *Coord. Chem. Rev. 367*, 18−64.

(2) Shimberg, G. D., Pritts, J. D., and Michel, S. L. J. (2018) Iron-Sulfur Clusters in Zinc Finger Proteins. *Methods Enzymol. 599*, 101−137.

(3) Jantz, D., Amann, B. T., Gatto, G. J., and Berg, J. M. (2004) The Design of Functional DNA-Binding Proteins Based on Zinc Finger Domains. *Chem. Rev. 104*, 789−800.

(4) Lee, S. J., and Michel, S. L. J. (2014) Structural Metal Sites in Nonclassical Zinc Finger Proteins Involved in Transcriptional and Translational Regulation. *Acc. Chem. Res. 47*, 2643−2650.

(5) Maret, W. (2012) New perspectives of zinc coordination environments in proteins. *J. Inorg. Biochem. 111*, 110−116.

(6) Miller, J., McLachlan, A. D., and Klug, A. (1985) Repetitive zinc-binding domains in the protein transcription factor IIIA from Xenopus oocytes. *EMBO J. 4*, 1609−1614.

(7) Laity, J. H., Lee, B. M., and Wright, P. E. (2001) Zinc finger proteins: new insights into structural and functional diversity. *Curr. Opin. Struct. Biol. 11*, 39−46.

(8) Searles, M. A., Lu, D., and Klug, A. (2000) The role of the central zinc fingers of transcription factor IIIA in binding to 5 S RNA. *J. Mol. Biol. 301*, 47−60.

(9) Klug, A. (2010) The Discovery of Zinc Fingers and Their Applications in Gene Regulation and Genome Manipulation. *Annu. Rev. Biochem. 79*, 213−231.

(10) Andreini, C., Banci, L., Bertini, I., and Rosato, A. (2006) Zinc through the Three Domains of Life. *J. Proteome. Res. 5*, 3173−3178.

(11) Andreini, C., Banci, L., Bertini, I., and Rosato, A. (2006) Counting the zinc-proteins encoded in the human genome. *J. Proteome. Res. 5*, 196−201.

(12) Bertini, I., Decaria, L., and Rosato, A. (2010) The annotation of full zinc proteomes. *JBIC, J. Biol. Inorg. Chem. 15*, 1071−1078.

(13) Krishna, S. S., Majumdar, I., and Grishin, N. V. (2003) Structural classification of zinc fingers. *Nucleic Acids Res. 31*, 532−550.

(14) Matthews, J. M., and Sunde, M. (2002) Zinc Fingers–Folds for Many Occasions. *IUBMB Life 54*, 351−355.

(15) Michalek, J. L., Besold, A. N., and Michel, S. L. (2011) Cysteine and histidine shuffling: mixing and matching cysteine and histidine residues in zinc finger proteins to afford different folds and function. *Dalton Trans. 40*, 12619−12632.

(16) Fu, M., and Blackshear, P. J. (2017) RNA-binding proteins in immune regulation: a focus on CCCH zinc finger proteins. *Nat. Rev. Immunol. 17*, 130−143.

(17) Maeda, K., and Akira, S. (2017) Regulation of mRNA stability by CCCH-type zinc-finger proteins in immune cells. *Int. Immunol. 29*, 149−155.

(18) Shimberg, G. D., Michalek, J. L., Oluyadi, A. A., Rodrigues, A. V., Zucconi, B. E., Neu, H. M., Ghosh, S., Sureschandra, K., Wilson, G. M., Stemmler, T. L., and Michel, S. L. J. (2016) Cleavage and polyadenylation specificity factor 30: An RNA-binding zinc-finger protein with an unexpected 2Fe−2S cluster. *Proc. Natl. Acad. Sci. U. S. A. 113*, 4700−4705.

(19) Yang, Q., and Doublié, S. (2011) Structural biology of poly(A) site definition. *Wiley Interdiscip. Rev.: RNA 2*, 732−747.

(20) Chan, S. L., Huppertz, I., Yao, C., Weng, L., Moresco, J. J., Yates, J. R., Ule, J., Manley, J. L., and Shi, Y. (2014) CPSF30 and Wdr33 directly bind to AAUAAA in mammalian mRNA 3′ processing. *Genes Dev. 28*, 2370−2380.

(21) Proudfoot, N. J. (2011) Ending the message: poly(A) signals then and now. *Genes Dev. 25*, 1770−1782.

(22) Chang, J. W., Yeh, H. S., and Yong, J. (2017) Alternative Polyadenylation in Human Diseases. *Endocrinol. Metab. (Seoul). 32*, 413−421.

(23) Thore, S., and Fribourg, S. (2019) Structural insights into the 3′-end mRNA maturation machinery: Snapshot on polyadenylation signal recognition. *Biochimie 164*, 105−110.

(24) Baxter, E. L., Jennings, P. A., and Onuchic, J. N. (2012) Strand swapping regulates the iron-sulfur cluster in the diabetes drug target mitoNEET. *Proc. Natl. Acad. Sci. U. S. A. 109*, 1955−1960.

(25) Conlan, A. R., Axelrod, H. L., Cohen, A. E., Abresch, E. C., Zuris, J., Yee, D., Nechushtai, R., Jennings, P. A., and Paddock, M. L. (2009) Crystal Structure of Miner1: The Redox-active 2Fe-2S Protein Causative in Wolfram Syndrome 2. *J. Mol. Biol. 392*, 143−153.

(26) Tamir, S., Paddock, M. L., Darash-Yahana-Baram, M., Holt, S. H., Sohn, Y. S., Agranat, L., Michaeli, D., Stofleth, J. T., Lipper, C. H., Morcos, F., Cabantchik, I. Z., Onuchic, J. N., Jennings, P. A., Mittler, R., and Nechushtai, R. (2015) Structure−function analysis of NEET proteins uncovers their role as key regulators of iron and ROS homeostasis in health and disease. *Biochim. Biophys. Acta, Mol. Cell Res. 1853*, 1294−1315.

(27) Wiley, S. E., Paddock, M. L., Abresch, E. C., Gross, L., van der Geer, P., Nechushtai, R., Murphy, A. N., Jennings, P. A., and Dixon, J. E. (2007) The Outer Mitochondrial Membrane Protein mitoNEET Contains a Novel Redox-active 2Fe-2S Cluster. *J. Biol. Chem. 282*, 23745−23749.

(28) Wiley, S. E., Murphy, A. N., Ross, S. A., van der Geer, P., and Dixon, J. E. (2007) MitoNEET is an iron-containing outer mitochondrial membrane protein that regulates oxidative capacity. *Proc. Natl. Acad. Sci. U. S. A. 104*, 5318−5323.

(29) Lin, J., Zhang, L., Lai, S., and Ye, K. (2011) Structure and molecular evolution of CDGSH iron-sulfur domains. *PLoS One 6*, e24790.

(30) Lipper, C. H., Karmi, O., Sohn, Y. S., Darash-Yahana, M., Lammert, H., Song, L., Liu, A., Mittler, R., Nechushtai, R., Onuchic, J. N., and Jennings, P. A. (2018) Structure of the human monomeric NEET protein MiNT and its role in regulating iron and reactive oxygen species in cancer cells. *Proc. Natl. Acad. Sci. U. S. A. 115*, 272−277.

(31) Cutone, A., Howes, B. D., Miele, A. E., Miele, R., Giorgi, A., Battistoni, A., Smulevich, G., Musci, G., and di Patti, M. C. (2016) Pichia pastoris Fep1 is a [2Fe-2S] protein with a Zn finger that displays an unusual oxygen-dependent role in cluster binding. *Sci. Rep. 6*, 31872.

(32) Sun, Y., Zhang, Y., Hamilton, K., Manley, J. L., Shi, Y., Walz, T., and Tong, L. (2018) Molecular basis for the recognition of the human AAUAAA polyadenylation signal. *Proc. Natl. Acad. Sci. U. S. A. 115*, E1419−E1428.

(33) Clerici, M., Faini, M., Muckenfuss, L. M., Aebersold, R., and Jinek, M. (2018) Structural basis of AAUAAA polyadenylation signal recognition by the human CPSF complex. *Nat. Struct. Mol. Biol. 25*, 135−138.

(34) Barabino, S. M., Hubner, W., Jenny, A., Minvielle-Sebastia, L., and Keller, W. (1997) The 30-kD subunit of mammalian cleavage and polyadenylation specificity factor and its yeast homolog are RNA-binding zinc finger proteins. *Genes Dev. 11*, 1703−1716.

(35) D'Souza, V., and Summers, M. F. (2004) Structural basis for packaging the dimeric genome of Moloney murine leukaemia virus. *Nature 431*, 586−590.

(36) Benhalevy, D., Gupta, S. K., Danan, C. H., Ghosal, S., Sun, H. W., Kazemier, H. G., Paeschke, K., Hafner, M., and Juranek, S. A. (2017) The Human CCHC-type Zinc Finger Nucleic Acid-Binding Protein Binds G-Rich Elements in Target mRNA Coding Sequences and Promotes Translation. *Cell Rep. 18*, 2979−2990.

(37) Schuler, W., Dong, C., Wecker, K., and Roques, B. P. (1999) NMR structure of the complex between the zinc finger protein NCp10 of Moloney murine leukemia virus and the single-stranded pentanucleotide d(ACGCC): comparison with HIV-NCp7 complexes. *Biochemistry 38*, 12984−12994.

(38) Tian, B., and Graber, J. H. (2012) Signals for pre-mRNA cleavage and polyadenylation. *Wiley Interdiscip. Rev.: RNA 3*, 385−396.

https://dx.doi.org/10.1021/acs.biochem.9b01065
Biochemistry 2020, 59, 970−982

(39) McDevitt, M. A., Hart, R. P., Wong, W. W., and Nevins, J. R. (1986) Sequences capable of restoring poly(A) site function define two distinct downstream elements. *EMBO J. 5*, 2907−2913.
(40) Gil, A., and Proudfoot, N. J. (1987) Position-dependent sequence elements downstream of AAUAAA are required for efficient rabbit beta-globin mRNA 3′ end formation. *Cell 49*, 399−406.
(41) Levitt, N., Briggs, D., Gil, A., and Proudfoot, N. J. (1989) Definition of an efficient synthetic poly(A) site. *Genes Dev. 3*, 1019−1025.
(42) diTargiani, R. C., Lee, S. J., Wassink, S., and Michel, S. L. (2006) Functional characterization of iron-substituted tristetraprolin-2D (TTP-2D, NUP475−2D): RNA binding affinity and selectivity. *Biochemistry 45*, 13641−13649.
(43) Shimberg, G. D., Ok, K., Neu, H. M., Splan, K. E., and Michel, S. L. J. (2017) Cu(I) Disrupts the Structure and Function of the Nonclassical Zinc Finger Protein Tristetraprolin (TTP). *Inorg. Chem. 56*, 6838−6848.
(44) George, G. N., George, S. J., and Bommannavar, A. S. E. (2001) *EXAFSPAK*. http://ssrl.slac.stanford.edu/exafspak.html.
(45) Ankudinov, A. L., and Rehr, J. J. (1997) Relativistic calculations of spin-dependent x-ray-absorption spectra. *Phys. Rev. B: Condens. Matter Mater. Phys. 56*, R1712−R1716.
(46) Cook, J. D., Kondapalli, K. C., Rawat, S., Childs, W. C., Murugesan, Y., Dancis, A., and Stemmler, T. L. (2010) Molecular details of the yeast frataxin-Isu1 interaction during mitochondrial Fe-S cluster assembly. *Biochemistry 49*, 8756−8765.
(47) Bencze, K., Kondapalli, K., and Stemmler, T. (2007) X-ray absorption spectroscopy. In *Applications of Physical Methods to Inorganic and Bioinorganic Chemistry* (Scott, R., and Lukehart, C., Eds.) pp 513−528, Wiley, Chichester, U.K.
(48) Cotelesage, J. J., Pushie, M. J., Grochulski, P., Pickering, I. J., and George, G. N. (2012) Metalloprotein active site structure determination: synergy between X-ray absorption spectroscopy and X-ray crystallography. *J. Inorg. Biochem. 115*, 127−137.
(49) Riggs-Gelasco, P. J., Stemmler, T. L., and Penner-Hahn, J. E. (1995) XAFS of dinuclear metal sites in proteins and model compounds. *Coord. Chem. Rev. 144*, 245−286.
(50) Mely, Y., De Rocquigny, H., Morellet, N., Roques, B. P., and Gérard, D. (1996) Zinc binding to the HIV-1 nucleocapsid protein: a thermodynamic investigation by fluorescence spectroscopy. *Biochemistry 35*, 5175−5182.
(51) Guo, J., and Giedroc, D. P. (1997) Zinc site redesign in T4 gene 32 protein: structure and stability of cobalt(II) complexes formed by wild-type and metal ligand substitution mutants. *Biochemistry 36*, 730−742.
(52) Bavoso, A., Ostuni, A., Battistuzzi, G., Menabue, L., Saladini, M., and Sola, M. (1998) Metal ion binding to a zinc finger peptide containing the Cys-X2-Cys-X4-His-X4-Cys domain of a nucleic acid binding protein encoded by the Drosophila Fw-element. *Biochem. Biophys. Res. Commun. 242*, 385−389.
(53) Abbehausen, C., Peterson, E. J., de Paiva, R. E., Corbi, P. P., Formiga, A. L., Qu, Y., and Farrell, N. P. (2013) Gold(I)-phosphine-N-heterocycles: biological activity and specific (ligand) interactions on the C-terminal HIVNCp7 zinc finger. *Inorg. Chem. 52*, 11280−11287.
(54) Berg, J. M., and Merkle, D. L. (1989) On the metal ion specificity of zinc finger proteins. *J. Am. Chem. Soc. 111*, 3759−3761.
(55) Clerici, M., Faini, M., Aebersold, R., and Jinek, M. (2017) Structural insights into the assembly and polyA signal recognition mechanism of the human CPSF complex. *eLife 6*, E33111.
(56) Herbst, R. W., Perovic, I., Martin-Diaconescu, V., O'Brien, K., Chivers, P. T., Pochapsky, S. S., Pochapsky, T. C., and Maroney, M. J. (2010) Communication between the zinc and nickel sites in dimeric HypA: metal recognition and pH sensing. *J. Am. Chem. Soc. 132*, 10338−10351.
(57) Clark-Baldwin, K., Tierney, D. L., Govindaswamy, N., Gruff, E. S., Kim, C., Berg, J., Koch, S. A., and Penner-Hahn, J. E. (1998) The Limitations of X-ray Absorption Spectroscopy for Determining the Structure of Zinc Sites in Proteins. When Is a Tetrathiolate Not a Tetrathiolate? *J. Am. Chem. Soc. 120*, 8401−8409.
(58) Hollerer, I., Grund, K., Hentze, M. W., and Kulozik, A. E. (2014) mRNA 3′end processing: A tale of the tail reaches the clinic. *EMBO Mol. Med. 6*, 16−26.
(59) Magyar, J. S., and Godwin, H. A. (2003) Spectropotentiometric analysis of metal binding to structural zinc-binding sites: accounting quantitatively for pH and metal ion buffering effects. *Anal. Biochem. 320*, 39−54.
(60) MacColl, R., Eisele, L. E., Stack, R. F., Hauer, C., Vakharia, D. D., Benno, A., Kelly, W. C., and Mizejewski, G. J. (2001) Interrelationships among biological activity, disulfide bonds, secondary structure, and metal ion binding for a chemically synthesized 34-amino-acid peptide derived from alpha-fetoprotein. *Biochim. Biophys. Acta, Gen. Subj. 1528*, 127−134.
(61) Krizek, B. A., Merkle, D. L., and Berg, J. M. (1993) Ligand variation and metal ion binding specificity in zinc finger peptides. *Inorg. Chem. 32*, 937−940.
(62) Lai, W. S., Carballo, E., Strum, J. R., Kennington, E. A., Phillips, R. S., and Blackshear, P. J. (1999) Evidence that tristetraprolin binds to AU-rich elements and promotes the deadenylation and destabilization of tumor necrosis factor alpha mRNA. *Mol. Cell. Biol. 19*, 4311−4323.
(63) Michel, S. L., Guerrerio, A. L., and Berg, J. M. (2003) Selective RNA binding by a single CCCH zinc-binding domain from Nup475 (Tristetraprolin). *Biochemistry 42*, 4626−4630.
(64) Brewer, B. Y., Malicka, J., Blackshear, P. J., and Wilson, G. M. (2004) RNA sequence elements required for high affinity binding by the zinc finger domain of tristetraprolin: conformational changes coupled to the bipartite nature of Au-rich MRNA-destabilizing motifs. *J. Biol. Chem. 279*, 27870−27877.
(65) Chakrabarti, M., and Hunt, A. G. (2015) CPSF30 at the Interface of Alternative Polyadenylation and Cellular Signaling in Plants. *Biomolecules 5*, 1151−1168.

https://dx.doi.org/10.1021/acs.biochem.9b01065
Biochemistry 2020, 59, 970−982